DMD Fast Forward. Published on June 18, 2007 as doi:10.1124/dmd.107.015248

DMD #15248

Interspecies comparisons of pharmacokinetics and pharmacodynamics of recombinant human erythropoietin (rHuEPO)

Sukyung Woo and William J. Jusko

Department of Pharmaceutical Sciences, School of Pharmacy and Pharmaceutical Sciences, State University of New York at Buffalo, Buffalo, New York

Running Title: Interspecies relationships of rHuEPO PK/PD

Corresponding Author:

William J. Jusko

Department of Pharmaceutical Sciences

School of Pharmacy and Pharmaceutical Sciences

565 Hochstetter Hall

State University of New York at Buffalo

Buffalo, NY 14260

Phone: (716) 645-2855 ext 225

FAX: (716) 645-3693

E-mail: wjjusko@buffalo.edu

Number of text pages: 16

Number of tables: 2

Number of figures: 6

Number of references: 40

Number of words in the Abstract: 215

Number of words in the Introduction: 541

Number of words in the Discussion: 1394

Abbreviations:

Pharmacokinetics, PK; pharmacodynamics, PD; erythropoietin, EPO; recombinant human erythropoietin, rHuEPO; clearance, CL; steady state volume of distribution, V_{ss}; central volume of distribution, V_c; erythropoietin receptor, EPOR; noncompartmental analysis, NCA; red blood cell, RBC; mature red blood cell, RBC_M;

DMD Fast Forward. Published on June 18, 2007 as DOI: 10.1124/dmd.107.015248
This article has not been copyedited and formatted. The final version may differ from this version.

ABSTRACT

Erythropoietin (EPO) has a highly conserved structure among mammals, and thus recombinant human erythropoietin (rHuEPO) has biological activity in various species. This study explores the interspecies relationships of the pharmacokinetics (PK) and pharmacodynamics (PD) of rHuEPO. The PK parameters such as clearance (*CL*) and volume of distribution (V_{ss}) after intravenous (i.v.) doses of rHuEPO were obtained in several species via non-compartmental analysis and were assessed using the traditional allometric approach. Also, PK/PD modeling of rHuEPO concentrations and responses (reticulocytes, RBC, and hemoglobin) was performed following a range of i.v. and s.c. doses in rats, monkeys, and humans. Nonlinear disposition (V_{max}, K_m), and s.c. absorption rate and bioavailability parameters of rHuEPO were examined. A cascade, indirect, lifespan PD model was applied to recover efficacy (S_{max}) and potency (SC_{50}) of rHuEPO on erythropoiesis, and erythroid cell lifespan parameters. Despite nonlinear rHuEPO disposition, *CL* and V_{ss} were highly correlated with body weight (R^2 >0.92) with allometric scaling exponents of 0.708 for *CL* and 0.853 for V_{ss}. The s.c. bioavailability increased with dose in monkey and human but appeared to be dose-independent in rats. A correlation between S_{max} or SC_{50} and body weight was not obvious. However, RBC lifespans obeyed allometric principles. Size dependence was found for PK and lifespan parameters, whereas pharmacologic parameters were independent of body weight.

INTRODUCTION

Recombinant human erythropoietin (rHuEPO) has been widely used clinically for treatment of anemia associated with chronic renal failure and chemotherapy. Erythropoietin (EPO) is the primary hormone of erythropoiesis and mainly synthesized in the kidney in response to hypoxia. Upon binding to its receptor (EPOR) on progenitor cells in the bone marrow, EPO stimulates proliferation and differentiation of erythroid cells, leading to an increase in reticulocytes followed by rises in RBC and hemoglobin (Hb) in the blood.

EPO is a glycosylated protein with molecular weight (MW) of 30.4 kDa. Amino acid sequences in the coding region of mature EPO protein shows a high degree of homology among mammals. The human EPO sequence is 91% homologous to monkey EPO, 85% to cat and dog EPO, and 80-82% to sheep, pig, mouse, and rat EPO (Wen et al., 1993). This explains the biological activity of rHuEPO that has been observed across species.

Interspecies similarities in structural, physiological, and biochemical properties result in allometric equations that characterize the dependency of biological variables on body weight (Dedrick, 1973; Mordenti, 1986). Allometric scaling has been widely used to predict pharmacokinetic (PK) parameters of small molecules, but has been applied to a limited extent to macromolecules. It is well accepted that interspecies scaling works best for drugs that are eliminated primarily by physical processes, i.e., biliary or renal excretion, compared to metabolism or drugs with nonlinear disposition. Because of their large molecular size (1-400 kDa), clearance mechanisms for proteins may be significantly different from small molecules, that is proteolysis, renal filtration and catabolism, and hepatic uptake via sugar-recognizing receptors (Braeckman, 1999). In addition, most macromolecules are endogenously present in the body, which may influence the disposition of exogenously given molecules. Effects of species

specificity and immune-mediated clearance on scaling preclinical data to humans has been reported (Richter et al., 1999). However, despite these factors that may complicate interspecies scaling of proteins, studies have shown that *CL* of proteins may be predicted with a reasonable accuracy from preclinical data (Mordenti et al., 1991; Mahmood, 2004; Tang and Mayersohn, 2006).

The assessment of PD among species is seldom carried out with mechanistic PK/PD models. These offer the opportunity to assess both pharmacologic (capacity, sensitivity) factors as well as systemic variables (biochemical, physiological). The former are likely to exhibit genetic differences while the latter are more apt to obey allometric principles (Lepist and Jusko, 2004).

In this study we evaluated the allometric relationships of PK and PD properties of rHuEPO in various animals and humans. The kinetic characteristics of rHuEPO include nonlinear PK, prolonged absorption and variable incomplete bioavailability upon SC administration, which has often been observed for other therapeutic protein drugs (Radwanski et al., 1998; Mager and Jusko, 2002) and can be a challenge in assessment of the allometry. In the presence of nonlinear kinetics, direct comparisons of PK parameters of interest such as clearance, volume of distribution and bioavailability are difficult because these values change with dose when calculated by traditional methods. Our laboratory has previously reported the PK/PD analysis of rHuEPO following i.v. and s.c. doses in rats, monkeys, and humans using comprehensive PK/PD models that share general common structures, thereby allowing interspecies comparisons of PK/PD parameters. To extend our findings additional information from the literature was included.

METHODS

CL and V_{ss} by noncompartmental analysis.

The PK data following i.v. administration of rHuEPO-alpha (hereafter rHuEPO) were obtained from the literature for various species including rats (Kato et al., 2001; Woo et al., 2006), rabbits (Yoon et al., 1997), monkeys (Ramakrishnan et al., 2003), dogs (Fu et al., 1988), sheep (Widness et al., 1996; McLennan et al., 2005), and humans (Ramakrishnan et al., 2004). The values of clearance (*CL*) and steady-state volume of distribution (V_{ss}) were calculated based on a noncompartmental approach (Gibaldi and Perrier, 1982). When the reference did not report the values but included time profiles of rHuEPO concentrations, the data were digitized and WinNonlin (Pharsight Corp., NC) was used to calculate the parameters with the noncompartmental analysis (NCA) option. Due to the nonlinearity, the values of *CL* and V_{ss} were calculated at each dosage.

PK and PD parameters by PK/PD modeling approach.

The PK and PD parameters of rHuEPO were obtained from rats (Woo et al., 2006), monkeys (Ramakrishnan et al., 2003), and humans (Ramakrishnan et al., 2004). Each study reported the parameter estimates by computational fittings using the PK and PD data from i.v. and s.c. administration of a wide dosage range of rHuEPO. A general structure of the PK/PD model of rHuEPO applied to the three species is shown in Figure 1. The PK model depicts nonlinear elimination (V_{max}, K_m) as well as s.c. absorption kinetics where the bioavailable fraction (*F*) of rHuEPO gets absorbed via a zero-order rate (k_0) followed by a first-order rate (k_a) from the injection site. The PD model mimics the process of erythropoiesis from bone marrow erythroid cells (*P1* and *P2*) to peripheral blood cells (*RET* and RBC_M). The PD model is based on cell lifespan concepts where the cell conversion from a predecessor to a successor is controlled

DMD Fast Forward. Published on June 18, 2007 as DOI: 10.1124/dmd.107.015248
This article has not been copyedited and formatted. The final version may differ from this version.

by its own lifespan (Krzyzanski et al., 1999). The mean lifespans of successive cell populations was represented by T_{P1}, T_{P2}, T_{RET}, and T_{RBC}. The RBC and Hb increase as rHuEPO stimulates the proliferation and differentiation of progenitor cells (S_{max}, SC_{50}), but a feedback regulatory mechanism prevents their excessive increase by inhibiting the production of progenitors (I_{max}, IC_{50}). Details about the PK/PD model equations were described in the original publications. Representative time profiles of the observed and predicted rHuEPO concentrations and reticulocytes in rats and humans are shown in Figure 2.

The PD parameters for rats and humans based on single dose studies were directly taken from the original articles. The PD data from monkey and two multiple-dose studies in humans were re-analyzed with the PD model used for rats (Woo et al., 2006). All computer fittings were performed by ADAPT II (Biomedical Simulation Resources, CA).

Allometric analysis

An allometric equation was used to relate PK or PD parameters of rHuEPO with body weight:

$$Y = a \cdot BW^{b}$$

where Y is the parameter of interest, BW is body weight in kilograms, a is the allometric coefficient, and b is the allometric exponent. In order to include a wide range of body weights, the RBC lifespans for other animals (Allison, 1960) were included.

RESULTS

Comparisons of *CL* and V_{ss} of rHuEPO.

Table 1 lists the body weights, ranges of dosages, *CL*, and V_{ss} for i.v. administration of rHuEPO from six species. Based on the NCA, sets of *CL* and V_{ss} exist for as many as the number of dosages evaluated and thus these values are presented as a range. Most studies have reported the nonlinear PK of rHuEPO, mainly characterized by a decrease in *CL* with increasing dose. With respect to V_{ss} across species, it appeared that the values were greater than plasma volume (i.e., 4.5% of body weight or 45 ml/kg) but less than about half of the extracellular water space volume (i.e., 27% of body weight or 270 ml/kg). Although there did not appear dose-dependency in V_{ss}, especially in small animals, the values in some species such as monkey, sheep, and humans showed changes for a wide range of dosages. They were not necessarily dose-related, but tended to be slightly higher at low and high doses compared to those in medium doses.

The interspecies relationships of *CL* and V_{ss} taken from all dosages of rHuEPO were described by allometric equations. As shown in Figure 3, a good correlation (R^2 > 0.92) between body weight and *CL* as well as V_{ss} was observed for rHuEPO. The parameters from humans were not included in the allometric analysis but predicted for a body weight of 70 kg from five animal species. The predicted values for *CL* (4.58 ml/h/kg) and V_{ss} (48.21 ml/kg) in humans were located within the range of observed values, close to ones obtained at the dosage of 150 IU/kg in humans. The exponent of *CL* (0.708) for rHuEPO was close to 0.75 whereas the exponent of V_{ss} (0.853) was slightly less than 1. The values of *CL* and V_{ss} for rHuEPO-beta in mice, rats, dogs (Bleuel et al., 1996), and humans (Halstenson et al., 1991), although they were not included in the

DMD Fast Forward. Published on June 18, 2007 as DOI: 10.1124/dmd.107.015248
This article has not been copyedited and formatted. The final version may differ from this version.

analysis, are also shown in Figure 3. In general, *CL* and V_{ss} for rHuEPO-beta fell closely near the regression line for those of rHuEPO except in mice whose values were higher than expected from the allometric equations.

Comparisons of PK parameters from PK modeling.

The PK parameters from the fittings were retrospectively compared for rats, monkeys, and humans. The PK data were described by a two-compartment model for rats and monkeys, and a one-compartment model for humans. Besides the Michaelis-Menten process, rats had a non-saturable elimination pathway (k_{el}). Figure 4 illustrates comparisons of nonlinearity parameters (V_{max}, K_m), central volume of distribution (V_c), and first-order absorption rate constant (k_a) among three species. The V_{max} was scaled with body weight ($R^2 > 0.98$) with the exponent of 0.504 while there was no correlation between K_m and body weight. The value of K_m was similar between monkeys and humans but much smaller in rats, probably due to having k_{el} in addition to saturable clearance in the PK model for rats. The central volume (V_c) was smaller than V_{ss} for rats and monkeys, which explains the need of the peripheral compartment in their PK model. The correlation between V_c and body weight was nearly unity ($R^2 > 0.999$) and V_c was almost directly proportional to body weight. The first-order absorption rate constants (k_a) associated with s.c. doses were negatively related to body weight. There was no obvious trend in the duration of the zero-order rate (13.5, 10, and 44-60 h) or the fraction absorbed via the zero-order process (68, 35, and 88%) among rats, monkeys, and humans.

Figure 5 displays the values of s.c. bioavailability vs. doses of rHuEPO obtained from simultaneous fittings of both i.v. and s.c. data in each species. The bioavailability observed in monkeys and humans clearly demonstrated a dose-dependant increase with

increasing doses and, more interestingly, resulted in 100% absorption at dosages > 2400 IU/kg of rHuEPO in both species. Unlike these two species, the s.c bioavailability in rats was constant (58%) and fell in the middle of the range.

Pharmacodynamic parameters of rHuEPO.

The mechanism-based PD model (Figure 1) was used to quantitatively describe the effects of rHuEPO including reticulocytes, RBC, and Hb. The typical response profiles of reticulocytes to rHuEPO administration are presented in Figure 2. The only difference in PD models for the three species was the component used to model the feedback inhibition (IC_{50}): reticulocytes for humans (Ramakrishnan et al., 2004), Hb for rats (Woo et al., 2006), and none for monkey (Ramakrishnan et al., 2003). For comparison purposes the PD data from the multiple-dosing studies in humans were modeled with Hb being the regulator of the feedback. For monkeys, however, the IC_{50} could not be estimated owing to very modest rebound phases observed in reticulocyte profiles.

The values of S_{max}, SC_{50}, and IC_{50} are provided in Table 2. Although the S_{max} in humans based on the single dose studies was higher than others, it ranged 1.5 – 2.0 across species. The values of SC_{50} varied from species to species: 26 – 45 mIU/ml for humans, 65 mIU/ml for rats, and 153 mIU/ml for monkeys, suggesting size independence. The values of IC_{50} with the same units were similar for rats (1.79 g/dl) and humans (2.88 g/dl).

Except for RBC lifespans which were usually fixed to the values from the literature, lifespan parameters for other RBC precursor cells were obtained through the computational fittings. As can be seen in Figure 6, the mean lifespans of P1 and RBC were well correlated to body weight ($R^2 > 0.8$), while the scaling of T_{RET} with weight was less obvious ($R^2 = 0.432$). Adding additional values from a wide range of species clearly

demonstrated that the RBC lifespans were dependent on their body size. Interestingly, the exponents of lifespan parameters were very similar, especially for T_{P1}, T_{P2}, and T_{RBC}, ranging from 0.124 to 0.148.

DISCUSSION

Pharmacokinetics. Interspecies scaling has been frequently used to predict human PK parameters based on animal data and is a useful tool for drug development. Application of allometric scaling for protein drugs is particularly interesting due to their different characteristics from small molecules. Mordenti et al (1991) showed excellent allometric relationships of *CL* and *V* for five proteins. Subsequent studies by Mahmood (2004) using 15 proteins, and Tang and Mayersohn (2006) using 10 proteins further indicated that *CL* of proteins may be scaled to body weight with reasonable consistency. The exponents for *CL* ranged widely 0.577 – 1.287. On average, clearance has an exponent of 0.75 and volume of 1.0 (Mordenti, 1986). Whether or not this is also applicable for *CL* of proteins is not known. Although *V* was not included in those studies, distribution of many biologic agents is often restricted to the vascular space due to their large molecular size, and thus, it can be expected that *V*, like blood volume, may be directly proportional to body weight.

For rHuEPO the exponent of V_{ss} (0.85) was less than 1 while the exponent of V_c (0.983) was almost 1. The difference between V_{ss} and V_c appeared to be larger in small animals, suggesting more distribution of rHuEPO outside the central compartments in small animals. Mahmood (2004) evaluated the interspecies scaling for *CL* of rHuEPO using rat (Kato et al., 2001), rabbit (Yoon et al., 1997) and dog (Fu et al., 1988), as well as rHuEPO-beta from mouse, rat and dog (Bleuel et al., 1996), and reported the exponents of 0.748 and 0.775. This slight difference from our study (0.708) is related to which value of *CL* was chosen from the original studies. Kato et al. (1997) obtained the allometric exponent of 0.70 for non-saturable clearance of rHuEPO from rat, dog, and human.

The major route of elimination for compounds greatly influences the predictability of human *CL* via allometry. As seen for small molecules, successful applications for renally eliminated macromolecules have been shown, including digoxin-specific Fab (Grene-Lerouge et al., 1996), interferon-α (Lave et al., 1995), Apo2L/TRAIL (Kelley et al., 2001), and recombinant CD4 (Mordenti et al., 1991). The disposition of rHuEPO has been assessed in context of ablation of kidneys (Emmanouel et al., 1984; Fu et al., 1988; Yoon et al., 1997), liver (Sytkowski, 1980; Widness et al., 1996), and bone marrow (Piroso et al., 1991; Chapel et al., 2001) in various animals. The results have consistently indicated that the kidneys contribute in a very minor fashion to rHuEPO elimination, i.e., only 4-7% of its overall elimination rate in animals and at most 10% in humans. The alteration of bone marrow function results in a significant change in rHuEPO PK, indicating that bone marrow may be a major route of rHuEPO elimination for low doses and contribute to its nonlinear PK via the receptor-mediated endocytosis. Although Michaelis-Menten kinetics does not directly reflect receptor-mediated drug elimination in bone marrow, the K_m value is similar to SC_{50} in rats (Woo et al., 2006) and sheep (Veng-Pedersen et al., 1999), suggesting that the saturable elimination and receptor binding may be closely related. The V_{max} correlated to body weight with an exponent of 0.504, suggesting a relationship of enzyme and/or receptor capacity.

The rate and extent of s.c. absorption of rHuEPO were compared based on results from three species. The characteristics of s.c. absorption of rHuEPO include a fast rising and flip-flop kinetics (Figure 2). In PK modeling, these features were captured by a zero-order followed by a first-order (k_a) input from the injection site. The k_a was found to be inversely correlated to body weight. This may be related to tissue size and blood flow

determinants of drug loss from the site of absorption. The zero-order process probably reflects rHuEPO absorption via the lymphatic pathway. This was based on studies that have shown involvement of lymphatics in the absorption of s.c. administered proteins and > 50% of an s.c. administered dose being absorbed by the regional lymphatics for molecules with MW > 16 kDa (Supersaxo et al., 1990; Porter and Charman, 2000). The PK model suggested > 68% of fraction absorbed via the zero-order input for rat and human, but lesser extent in monkey (35%). The contribution of the lymphatics to absorption of s.c. rHuEPO has been measured in sheep as > 75% of the administered dose (McLennan et al., 2005). The rate and bioavailability of s.c. absorption are influenced by the site of injection (Jensen et al., 1994) since regional lymphatic flow is highly dependent on the density of lymphatic vessels and frequency of muscle movement. This may explain why the duration of zero-order input and fraction of absorbed dose via the zero-order were not correlated to body size but are rather specific to species. A similar reason may indicate why bioavailability was independent of body weight. Bioavailability has been cited as a difficult parameter to predict from preclinical data (Mahmood, 2000; Tang and Mayersohn, 2006). The bioavailability for monkey and human varied with dosages < 2400 IU/kg but above that complete absorption was observed. The cause of incomplete s.c. bioavailability of rHuEPO is not known. The s.c. administration of rHuEPO encapsulated in liposomes produces almost three times higher lymph concentrations and bioavailability of rHuEPO (Moriya et al., 1997), suggesting that liposomes may protect rHuEPO from enzymatic degradation during absorption or transport into the circulation through the lymphatic pathway.

Pharmacodynamics. Erythropoiesis involves a series of cell proliferation and

differentiation steps from hematopoietic stem cells through the mature RBC. Since erythroid cells in the bone marrow were not individually measured, these cells were lumped into two subgroups in the PD modeling based on their similar characteristics, mainly dependence on EPO. Direct experimental measurements on survival half-lives of these RBC precursors are not available in the literature, and thus their lifespan values relied on the estimates from the PD modeling. Biological time periods (e.g., circulation time, maximum lifespan potential) tend to have an exponent of 0.25 (Mordenti, 1986). Based on the results from rat, monkey and human, the cell lifespans appeared to be dependent of body size. The exponents (0.124 ~ 0.148) were less than 0.25, but their slopes were very similar each other. Interspecies scaling of RBC lifespan based on a rich data set from diverse sources supported this finding.

Little is known about allometric relationships in PD. Few studies have reported allometric scaling of PD related parameters via modeling approaches (Gronert et al., 1995; Lepist and Jusko, 2004). As expected, the pharmacologic parameters of rHuEPO (S_{max} and SC_{50}) did not followed allometric principles, but may be more related to other factors such as receptor density and/or structural homology of EPO or EPOR between species. However, the sequence homology of EPO alone was not enough to explain these observations.

Interspecies comparisons of the PK/PD of rHuEPO may provide insights into the selection of animal models to study rHuEPO or its analogues. Rats appear to be a suitable preclinical small animal model for rHuEPO kinetics and dynamics. The PK/PD properties observed in rats were qualitatively similar to those observed from humans except for dose-dependent bioavailability. The RBC lifespan of rat (60 days) is a half of that of 120

days in humans. Other cell lifespans were also estimated to be about half of those for humans. However, changes in hematological baselines in rats with age add complexity in model development and interpretation of results (Woo et al., 2006). In spite of the high EPO homology (91%), monkeys well reflect the PK of rHuEPO for humans, especially in s.c. bioavailability, compared to the PD. The tolerance/rebound phenomenon observed in monkeys (Ramakrishnan et al., 2003) was not as prominent as in rats or humans, resulting in no need of the IC_{50}. Sheep are often used as a developmental animal model for erythropoiesis, probably due to the fact that sheep have almost the same lifespans of reticulocytes and RBC, and resemble developmental erythropoiesis in humans (Moritz et al., 1997).

We examined interspecies comparisons of PK and PD of rHuEPO via non-compartmental and mechanism-based PK/PD modeling approaches. Based on our findings, despite nonlinear PK behavior of rHuEPO, CL and V_{ss} were highly correlated with body weight. Bioavailability of rHuEPO following s.c. administration was dependent on dosage rather than body size. The pharmacologic parameters S_{max} and SC_{50} appeared to be species specific, but system parameters for RBC and precursor lifespans generally obeyed principles of allometry. The assessment of PD among species with mechanistic PK/PD models provided the opportunity to separate pharmacologic factors from systemic variables that are not dependent on drugs. This accumulating experience with PK/PD of rHuEPO will certainly help to understand PK/PD characteristics of EPO analogues and mimetics and facilitate their drug development processes.

REFERENCES

Allison AC (1960) Turnovers of erythrocytes and plasma proteins in mammals. *Nature* **188**:37-40.

Bleuel H, Hoffmann R, Kaufmann B, Neubert P, Ochlich PP and Schaumann W (1996) Kinetics of subcutaneous versus intravenous epoetin-beta in dogs, rats and mice. *Pharmacology* **52**:329-338.

Braeckman R (1999) Pharmacokinetics and pharmacodynamics of protein therapeutics, in *Peptide and Protein Drug Analysis* (Reid R ed) pp 633-669, University of British Columbia, Vancouver.

Chapel S, Veng-Pedersen P, Hohl RJ, Schmidt RL, McGuire EM and Widness JA (2001) Changes in erythropoietin pharmacokinetics following busulfan-induced bone marrow ablation in sheep: evidence for bone marrow as a major erythropoietin elimination pathway. *J Pharmacol Exp Ther* **298**:820-824.

Dedrick RL (1973) Animal scale-up. *J Pharmacokinet Biopharm* **1**:435-461.

Emmanouel DS, Goldwasser E and Katz AI (1984) Metabolism of pure human erythropoietin in the rat. *Am J Physiol* **247**:F168-176.

Fu JS, Lertora JJ, Brookins J, Rice JC and Fisher JW (1988) Pharmacokinetics of erythropoietin in intact and anephric dogs. *J Lab Clin Med* **111**:669-676.

Gibaldi M and Perrier D (1982) *Pharmacokinetics*. Marcel Dekker, New York.

Grene-Lerouge NA, Bazin-Redureau MI, Debray M and Scherrmann JM (1996) Interspecies scaling of clearance and volume of distribution for digoxin-specific Fab. *Toxicol Appl Pharmacol* **138**:84-89.

Gronert GA, Fung DL, Jones JH, Shafer SL, Hildebrand SV and Disbrow EA (1995)

Allometry of pharmacokinetics and pharmacodynamics of the muscle relaxant metocurine in mammals. *Am J Physiol* **268**:R85-91.

Halstenson CE, Macres M, Katz SA, Schnieders JR, Watanabe M, Sobota JT and Abraham PA (1991) Comparative pharmacokinetics and pharmacodynamics of epoetin alfa and epoetin beta. *Clin Pharmacol Ther* **50**:702-712.

Jensen JD, Jensen LW and Madsen JK (1994) The pharmacokinetics of recombinant human erythropoietin after subcutaneous injection at different sites. *Eur J Clin Pharmacol* **46**:333-337.

Kato M, Kamiyama H, Okazaki A, Kumaki K, Kato Y and Sugiyama Y (1997) Mechanism for the nonlinear pharmacokinetics of erythropoietin in rats. *J Pharmacol Exp Ther* **283**:520-527.

Kato M, Okano K, Sakamoto Y, Miura K, Uchimura T and Saito K (2001) Pharmacokinetics and pharmacodynamics of recombinant human erythropoietin in rats. *Arzneimittel-Forschung.* **51**:91-95.

Kelley SK, Harris LA, Xie D, Deforge L, Totpal K, Bussiere J and Fox JA (2001) Preclinical studies to predict the disposition of Apo2L/tumor necrosis factor-related apoptosis-inducing ligand in humans: characterization of in vivo efficacy, pharmacokinetics, and safety. *J Pharmacol Exp Ther* **299**:31-38.

Krzyzanski W, Ramakrishnan R and Jusko WJ (1999) Basic pharmacodynamic models for agents that alter production of natural cells. *J Pharmacokinet Biopharm* **27**:467-489.

Lave T, Levet-Trafit B, Schmitt-Hoffmann AH, Morgenroth B, Richter W and Chou RC (1995) Interspecies scaling of interferon disposition and comparison of allometric

scaling with concentration-time transformations. *J Pharm Sci* **84**:1285-1290.

Lepist EI and Jusko WJ (2004) Modeling and allometric scaling of s(+)-ketoprofen pharmacokinetics and pharmacodynamics: a retrospective analysis. *J Vet Pharmacol Ther* **27**:211-218.

Mager DE and Jusko WJ (2002) Receptor-mediated pharmacokinetic/pharmacodynamic model of interferon-beta 1a in humans. *Pharm Res* **19**:1537-1543.

Mahmood I (2000) Can absolute oral bioavailability in humans be predicted from animals? A comparison of allometry and different indirect methods. *Drug Metabol Drug Interact* **16**:143-155.

Mahmood I (2004) Interspecies scaling of protein drugs: prediction of clearance from animals to humans. *J Pharm Sci* **93**:177-185.

McLennan DN, Porter CJH, Edwards GA, Martin SW, Heatherington AC and Charman SA (2005) Lymphatic absorption is the primary contributor to the systemic availability of epoetin alfa following subcutaneous administration to sheep. *J Pharmacol Exp Ther* **313**:345-351.

Mordenti J (1986) Man versus beast: pharmacokinetic scaling in mammals. *J Pharm Sci* **75**:1028-1040.

Mordenti J, Chen SA, Moore JA, Ferraiolo BL and Green JD (1991) Interspecies scaling of clearance and volume of distribution data for five therapeutic proteins. *Pharm Res* **8**:1351-1359.

Moritz KM, Lim GB and Wintour EM (1997) Developmental regulation of erythropoietin and erythropoiesis. *American Journal of Physiology.* **273**:R1829-1844.

Moriya H, Maitani Y, Shimoda N, Takayama K and Nagai T (1997) Pharmacokinetic and

pharmacological profiles of free and liposomal recombinant human erythropoietin after intravenous and subcutaneous administrations in rats. *Pharmaceutical Research.* **14**:1621-1628.

Piroso E, Erslev AJ, Flaharty KK and Caro J (1991) Erythropoietin life span in rats with hypoplastic and hyperplastic bone marrows. *Am J Hematol* **36**:105-110.

Porter CJ and Charman SA (2000) Lymphatic transport of proteins after subcutaneous administration. *J Pharm Sci* **89**:297-310.

Radwanski E, Chakraborty A, Van Wart S, Huhn RD, Cutler DL, Affrime MB and Jusko WJ (1998) Pharmacokinetics and leukocyte responses of recombinant human interleukin-10. *Pharm Res* **15**:1895-1901.

Ramakrishnan R, Cheung WK, Farrell F, Joffee L and Jusko WJ (2003) Pharmacokinetic and pharmacodynamic modeling of recombinant human erythropoietin after intravenous and subcutaneous dose administration in cynomolgus monkeys. *J Pharmacol Exp Ther* **306**:324-331.

Ramakrishnan R, Cheung WK, Wacholtz MC, Minton N and Jusko WJ (2004) Pharmacokinetic and pharmacodynamic modeling of recombinant human erythropoietin after single and multiple doses in healthy volunteers. *J Clin Pharmacol* **44**:991-1002.

Richter WF, Gallati H and Schiller C-D (1999) Animal pharmacokinetics of the tumor necrosis factor receptor-immunoglobulin fusion protein lenercept and their extrapolation to humans. *Drug Metab Dispos* **27**:21-25.

Supersaxo A, Hein WR and Steffen H (1990) Effect of molecular weight on the lymphatic absorption of water-soluble compounds following subcutaneous

administration. *Pharm Res* **7**:167-169.

Sytkowski AJ (1980) Denaturation and renaturation of human erythropoietin. *Biochem Biophys Res Commun* **96**:143-149.

Tang H and Mayersohn M (2006) A global examination of allometric scaling for predicting human drug clearance and the prediction of large vertical allometry. *J Pharm Sci* **95**:1783-1799.

Veng-Pedersen P, Widness JA, Pereira LM, Schmidt RL and Lowe LS (1999) A comparison of nonlinear pharmacokinetics of erythropoietin in sheep and humans. *Biopharm Drug Dispos* **20**:217-223.

Wen D, Boissel JP, Tracy TE, Gruninger RH, Mulcahy LS, Czelusniak J, Goodman M and Bunn HF (1993) Erythropoietin structure-function relationships: high degree of sequence homology among mammals. *Blood* **82**:1507-1516.

Widness JA, Veng-Pedersen P, Schmidt RL, Lowe LS, Kisthard JA and Peters C (1996) In vivo 125I-erythropoietin pharmacokinetics are unchanged after anesthesia, nephrectomy and hepatectomy in sheep. *J Pharmacol Exp Ther* **279**:1205-1210.

Woo S, Krzyzanski W and Jusko WJ (2006) Pharmacokinetic and pharmacodynamic modeling of recombinant human erythropoietin after intravenous and subcutaneous administration in rats. *J Pharmacol Exp Ther* **319**:1297-1306.

Yoon WH, Park SJ, Kim IC and Lee MG (1997) Pharmacokinetics of recombinant human erythropoietin in rabbits and 3/4 nephrectomized rats. *Research Communications in Molecular Pathology & Pharmacology* **96**:227-240.

FOOTNOTES

This work was supported by NIH Grant GM 57980

Legends to Figures

Figure 1. Scheme of the PK/PD model for rHuEPO. The rHuEPO dose enters the central compartment via intravenous injection (D_{IV}) or a combination of first and zero-order inputs (k_a+k_0) following subcutaneous administration (D_{SC}). The rHuEPO in the central compartment (A_{EPO}) can distribute to peripheral tissue compartment (A_T) and be eliminated via saturable (V_{max}, K_m) and/or linear (k_{el}) elimination pathways. The drug acts on erythroid progenitor cells (*P1*) that eventually undergo a series of differentiations into erythroblasts (*P2*), reticulocytes (*RET*), and mature RBC (RBC_M). Other symbols are defined in the text.

Figure 2. Time profiles of the plasma concentrations of rHuEPO and reticulocyte counts following s.c. administration of rHuEPO at various dosages in rats (*top*; 450, 1350, and 4050 IU/kg) and humans (*bottom*; 450, 900, and 1800 IU/kg).

Figure 3. Allometric scaling of clearance (*top*) and volume of distribution (*bottom*) for i.v. doses of rHuEPO (●) across species. The observed values for humans (○) were not included in the regression. Each symbol represents *CL* or V_{ss} obtained by noncompartmental analysis at each single dose. The values of *CL* or V_{ss} for rHuEPO-beta (▲) were not included in the regression.

Figure 4. Allometric relationships of PK parameter estimates from the computational fittings: Michaelis-Menten capacity (V_{max}) and affinity (K_m) constants, central volume (V_c), and first-order absorption rate constant (k_a) *vs.* body weight.

Figure 5. Bioavailability *vs.* dose following s.c. administration of rHuEPO in three species.

Figure 6. Log-log representations of allometric relationships for cell lifespans of RBC

precursors (*top*) and RBC (*bottom*) vs. body weight.

DMD Fast Forward. Published on June 18, 2007 as DOI: 10.1124/dmd.107.015248
This article has not been copyedited and formatted. The final version may differ from this version.

Table 1. Comparisons of rHuEPO pharmacokinetics obtained via noncompartmental analysis in various species after i.v. doses.

Species	***BW (kg)***	***Doses (IU/kg)***	***CL (ml/h/kg)***	***V_{ss} (ml/kg)***
Rat	0.346 (0.31 – 0. 36)	450 – 4050 (3[a])	12.97 – 16.03	115 – 118
	0.211 (0.2 – 0.222)	1, 5, 25 μg/kg [b] (3)	19.6 – 29.4	108 – 123
Rabbit	2.37 (2.38 – 2.67)	1000 – 10000 (3)	9.9 – 13.98	52.4 – 59.1
Monkey	3.2[c]	500 – 4000 (3)	6.65 – 18.11	59.8 – 121
Dog	11 (9 – 14)	200000 cpm/kg[d] (1)	11	142
Sheep	29.4	0.052 – 0.16[d] (1)	37.73	105
	50 (40 – 60)	10 – 1000 (3)	4.46 – 12.3	48.3 – 72
Human	70 (56 – 89)	10 – 1000 (5)	3.70 – 14.68	39.5 – 89.0

[a] The number of dosages evaluated in the original study.

[b] Equivalent to 180, 900, and 4500 IU/kg

[c] Mean body weight for male cynomolgus monkeys (Allison, 1960)

[d] ^{125}I-rHuEPO was used

Table 2. Comparisons of pharmacologic parameters of rHuEPO.

Species	S_{max}	SC_{50} **(mIU/ml)**	IC_{50}
Rat[a]	1.87	65.37	1.79 g/dl[b]
Monkey[c]	1.92	153	
Human[a]	4.25	26.53	38.71×10^{10} cells/L[d]
Human[e]	1.53	45	2.88 g/dl[b]

[a] Taken from the original study.

[b] Represents as unit of hemoglobin.

[c] Remodeled PD data from Ramakrishnan et al. (2003).

[d] Represented as reticulocyte units.

[e] Remodeled PD data from multiple dosing studies (Ramakrishnan et al., 2004).

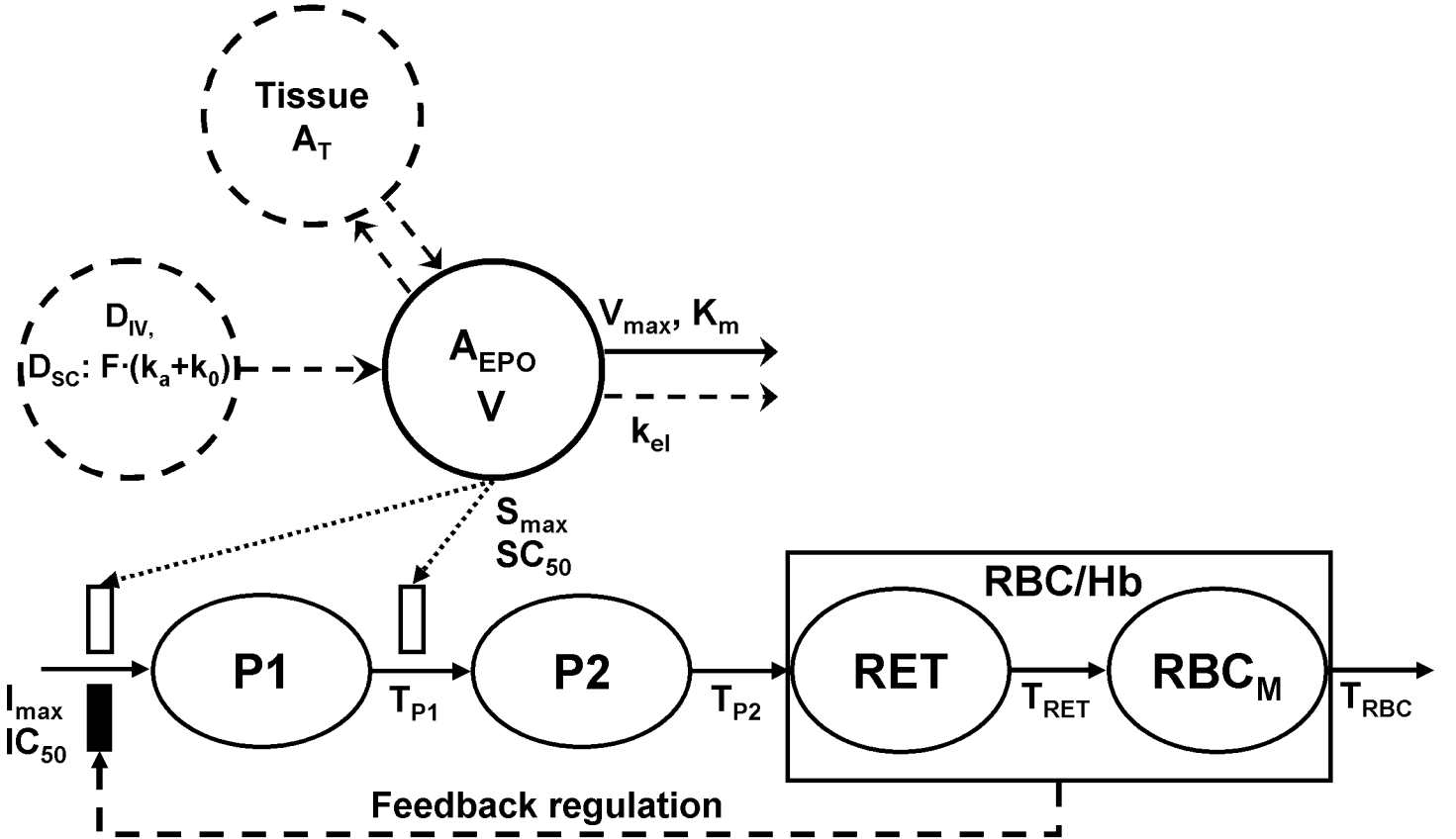
Tissue
A_T
D_{IV},
D_{SC}: $F \cdot (k_a + k_0)$
A_{EPO}
V
V_{max}, K_m
k_{el}
S_{max}
SC_{50}
P1
P2
RBC/Hb
RET
RBC_M
I_{max}
IC_{50}
T_{P1}
T_{P2}
T_{RET}
T_{RBC}
Feedback regulation

Figure 1

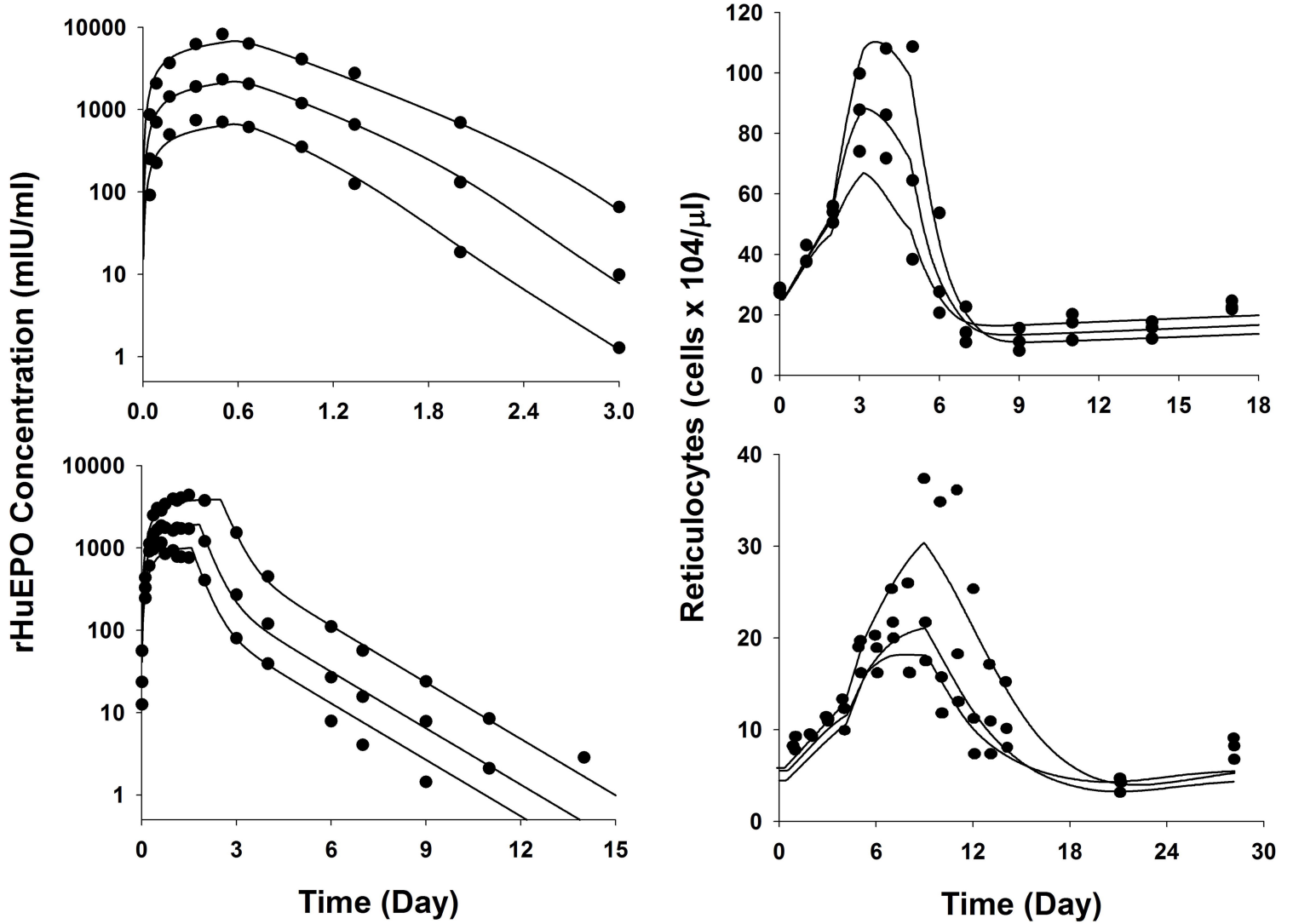
rHuEPO Concentration (mIU/ml)
10000
1000
100
10
1
0.0
0.6
1.2
1.8
2.4
3.0
10000
1000
100
10
1
0
3
6
9
12
15
Time (Day)
Reticulocytes (cells x 104/μl)
120
100
80
60
40
20
0
0
3
6
9
12
15
18
40
30
20
10
0
0
6
12
18
24
30
Time (Day)

Figure 2

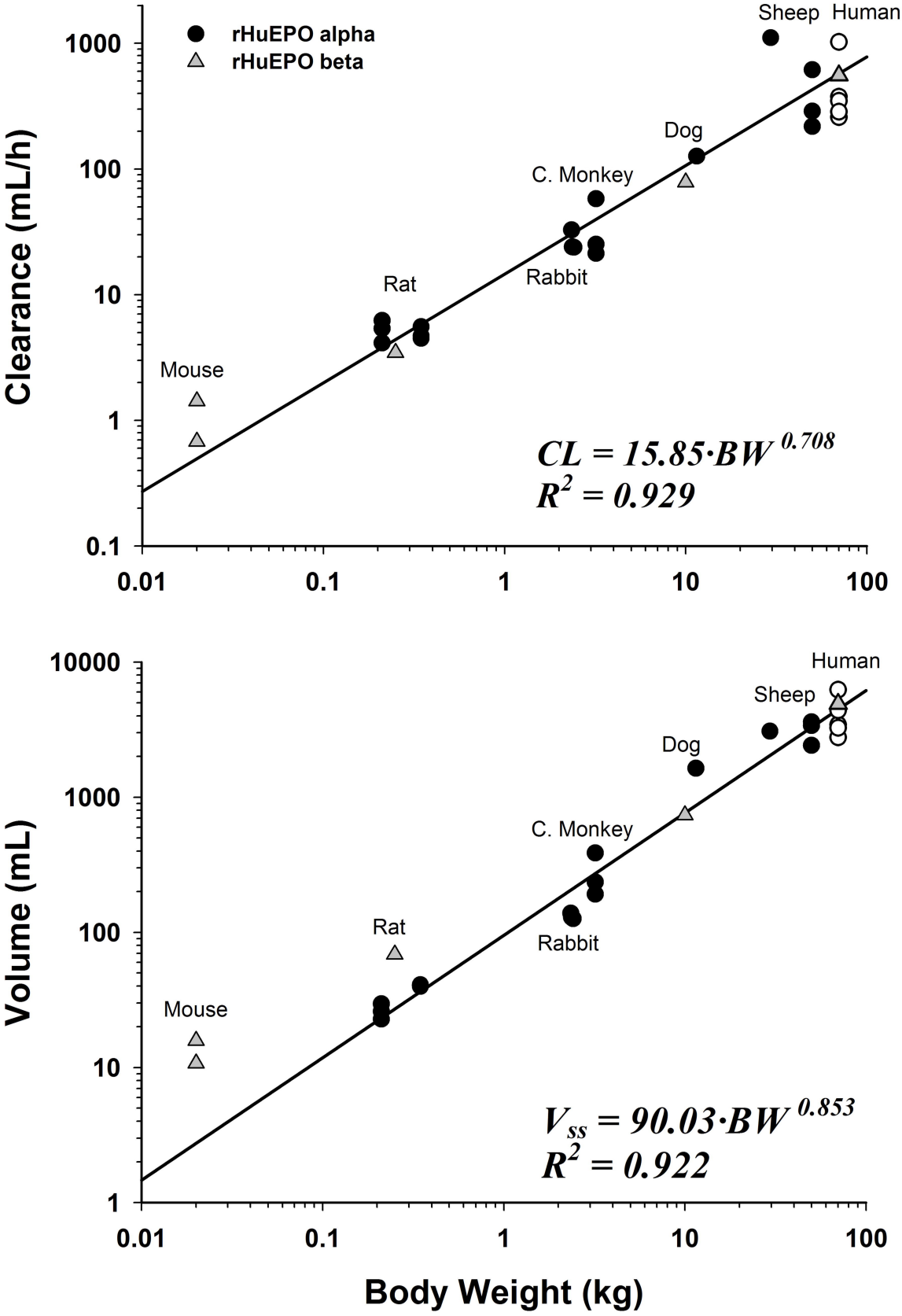
rHuEPO alpha
rHuEPO beta
Clearance (mL/h)
1000
100
10
1
0.1
0.01
0.1
1
10
100
Sheep
Human
Dog
C. Monkey
Rabbit
Rat
Mouse
$CL = 15.85 \cdot BW^{0.708}$
$R^2 = 0.929$
Volume (mL)
10000
1000
100
10
1
Human
Sheep
Dog
C. Monkey
Rat
Rabbit
Mouse
$V_{ss} = 90.03 \cdot BW^{0.853}$
$R^2 = 0.922$
Body Weight (kg)

Figure 3

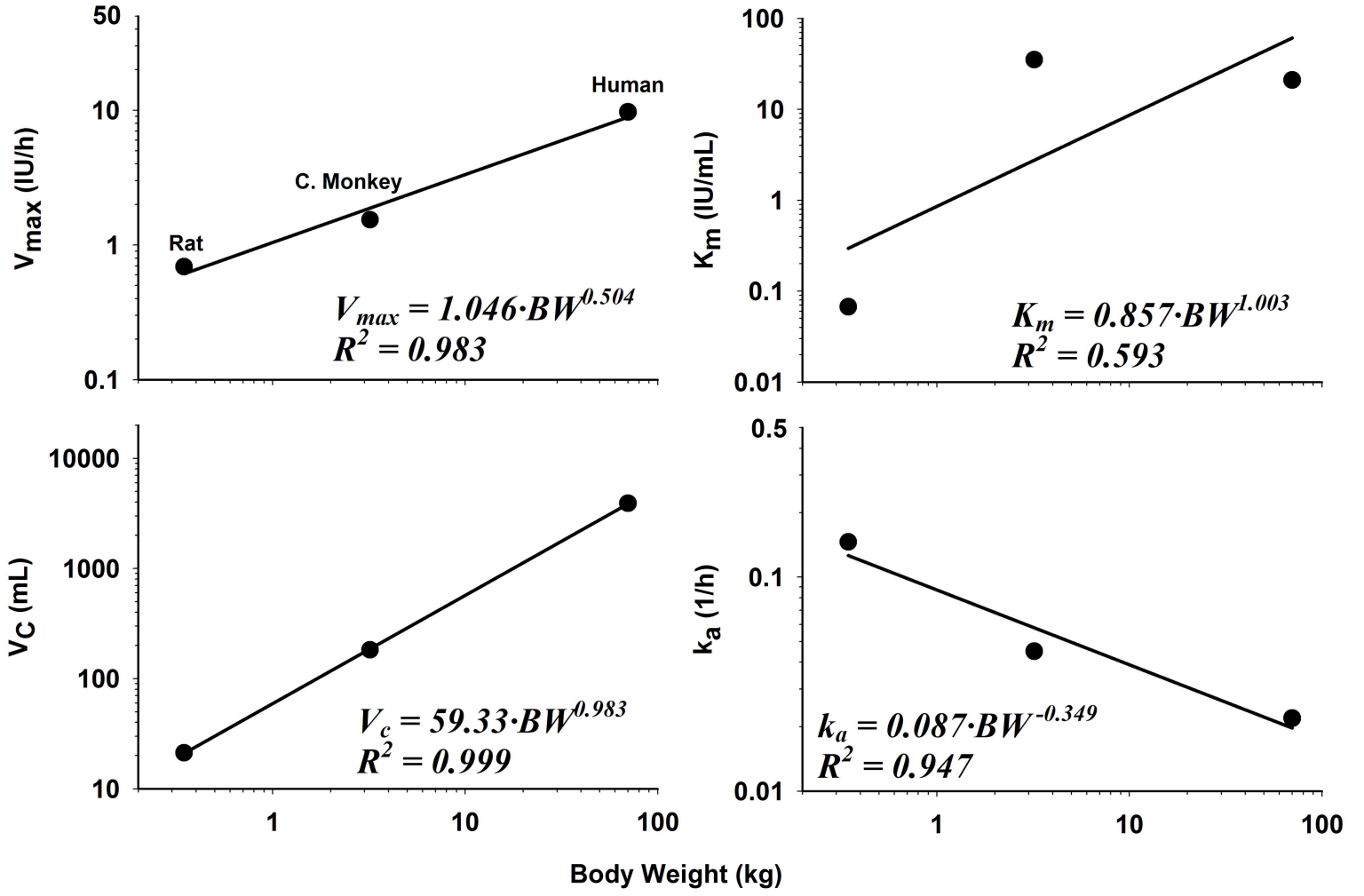
50
10
1
0.1
Vmax (IU/h)
Human
C. Monkey
Rat
$V_{max} = 1.046 \cdot BW^{0.504}$
$R^2 = 0.983$
100
10
1
0.1
0.01
Km (IU/mL)
$K_m = 0.857 \cdot BW^{1.003}$
$R^2 = 0.593$
10000
1000
100
10
VC (mL)
$V_c = 59.33 \cdot BW^{0.983}$
$R^2 = 0.999$
0.5
0.1
0.01
ka (1/h)
$k_a = 0.087 \cdot BW^{-0.349}$
$R^2 = 0.947$
1
10
100
Body Weight (kg)

Figure 4

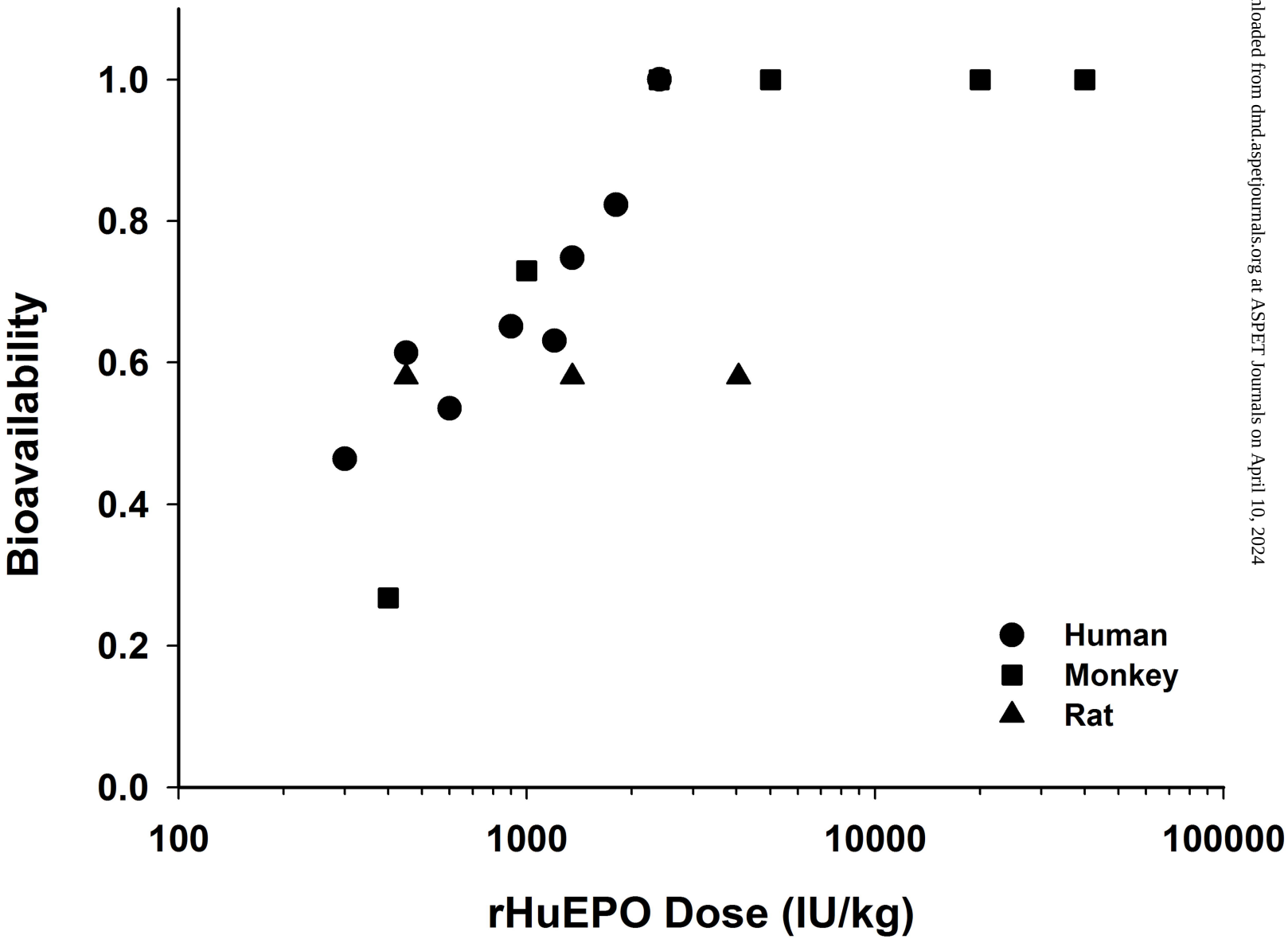

Figure 5

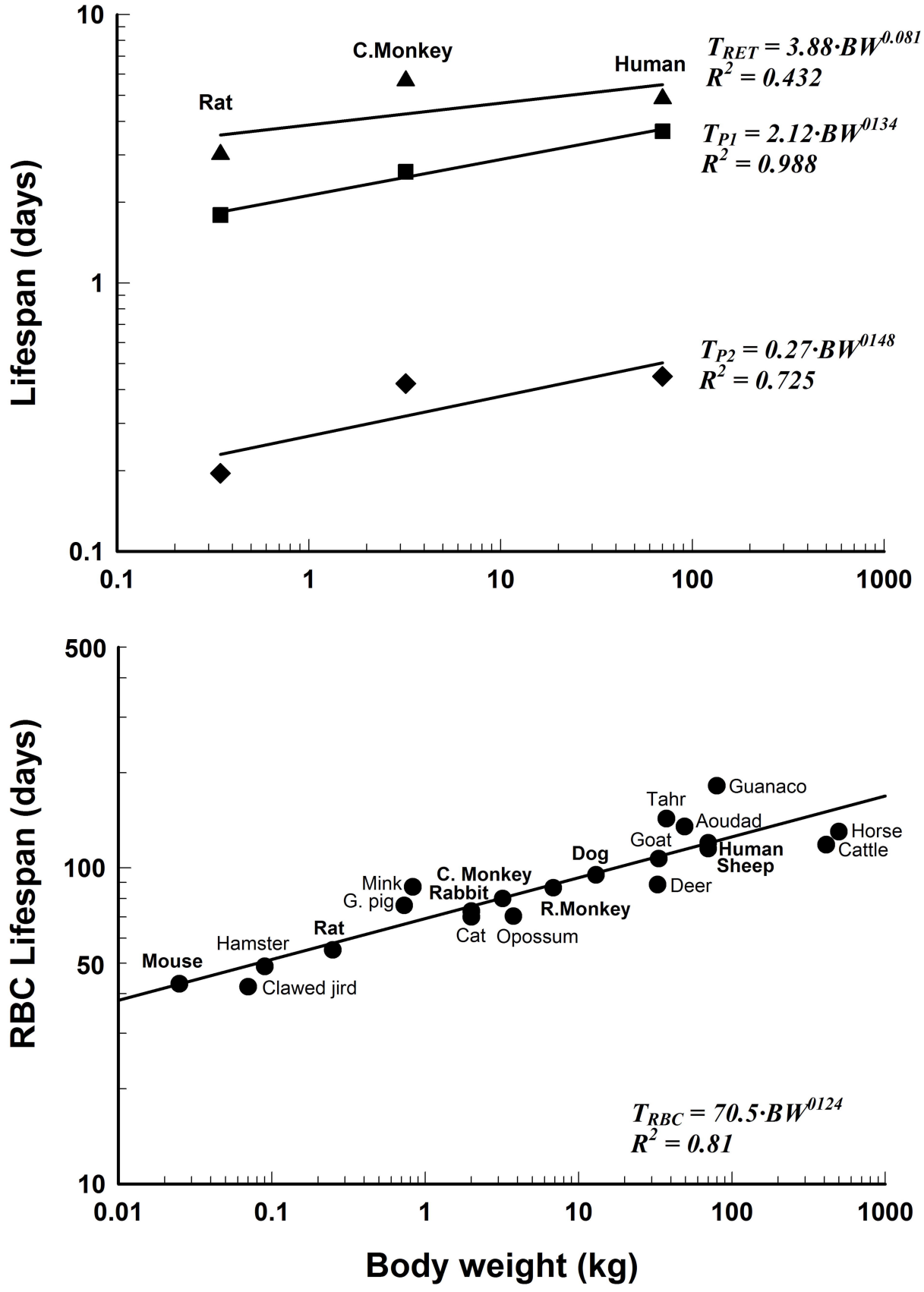
10
1
0.1
Lifespan (days)
C.Monkey
Human
Rat
$T_{RET} = 3.88 \cdot BW^{0.081}$
$R^2 = 0.432$
$T_{P1} = 2.12 \cdot BW^{0134}$
$R^2 = 0.988$
$T_{P2} = 0.27 \cdot BW^{0148}$
$R^2 = 0.725$
0.1
1
10
100
1000
500
100
50
10
RBC Lifespan (days)
Guanaco
Tahr
Aoudad
Goat
Horse
Cattle
Human
Sheep
Dog
Deer
Mink
G. pig
C. Monkey
Rabbit
R.Monkey
Cat
Opossum
Rat
Hamster
Mouse
Clawed jird
$T_{RBC} = 70.5 \cdot BW^{0124}$
$R^2 = 0.81$
0.01
0.1
1
10
100
1000
Body weight (kg)

Figure 6